

APPLICATION OF DIFFERENT NUMERICAL TOOLS AND NUMERICAL METHODS FOR PREDICTION OF HEAT EXCHANGER RAMAIR-CONCEPTS FOR HYBRID ELECTRIC PROPULSION AIRCRAFT CONFIGURATIONS

A. - R. Hübner¹, J. Kirz², K. Weinman³

1,2German Aerospace Center (DLR), Institute of Aerodynamics and Flow Technology Lilienthalplatz 7, 38108 Braunschweig, Germany Email: Andreas.Huebner@dlr.de, Jochen.Kirz@dlr.de

³German Aerospace Center (DLR), Institute of Aerodynamics and Flow Technology Bunsenstraße 10, 37073 Göttingen, Germany Email: Keith.Weinman@dlr.de

Abstract

Hybrid-electric propulsion concepts are utilized to satisfy the challenge of emission reduction in Aviation. Fuel cell systems are an integral component of hybrid propulsion systems. Heat exchangers are required to dissipate the waste heat produced by the fuel cell. Heat exchanger integration has an impact on the aircraft aerodynamics which in turn influences the flow through the cooler duct. This paper presents the application of a body force method implemented in the Flowsimulator Framework of the DLR-TAU code to simulate a heat exchanger system designed to be retro-fitted into the Dornier Do228 aircraft. The main focus here is the application, comparison and assessment of the heat exchanger method using both fixed values for the pressure drop and heat flux as well as a 3D Darcy-Forchheimer pressure drop model implemented within the DLR-TAU code.

Geometrical sensitivity studies of a generic RamAir concept are presented to get a detailed understanding of the flow characteristics of an integrated heat exchanger. Furthermore, the influence of the heat exchanger boundary conditions on the overall aerodynamic behavior of such an isolated cooler concept is evaluated. Within these examinations the impact of a grid refinement on the heat exchanger performance is analyzed. The influence of the different heat exchanger modeling approaches on the aerodynamic performance are examined and the capabilities of the new Darcy-Forchheimer approach are shown with some examples. The method is able to better capture the physics and allows new configurations to be investigated with greater geometric variability than before. As a result, the influence of the nozzle length and also the diffuser length is discussed and evaluated.

Keywords: Heat exchanger, numerical simulation, DLR-TAU code, body force modeling

Nomenclature

Α	cross-sectional area	m²	HEP	Hybrid-Electric Propulsion	
BFHEX	Body Force Heat Exchanger method		HEX	heat exchanger	-
C_D	drag coefficient	-	1	unit vector	-
CFD	Computational Flight Dynamics	-	N	number of grid points	-
C_{Fx}	skin friction coefficient in x-direction	-	U_{∞} (U)	freestream velocity (ref.)	m/s
\mathcal{C}_L	lift coefficient	-	V_{x}	velocity in x-direction	m/s
C_{My}	pitching moment coefficient	-	ṁ	mass flow rate	kg/s
C_p	static pressure coefficient	-	p_{∞}	static pressure (ref.)	Pa
DLR	German Aerospace Center		\dot{q} (qdot)	heat flux	W
D	Darcy coefficient	Pa·s/m²	T_{∞}	reference temperature (ref.)	K
F	Forchheimer coefficient	kg/m ⁴	α	angle of attack	0
FL	flight level	-	ρ	density	kg/m³
\vec{f}	momentum source term	Pa/m	Δp	pressure drop	Pa
f_0	Energy source term	W			

1. Introduction

A reduction of net greenhouse gas emissions by at least 55% by 2030 in comparison with the 1990 levels was formulated within the European Green Deal [1]. Currently the aeronautics is responsible for about 3.3% of the total CO2 emissions. In order to reduce the CO2 emissions for aircraft new propulsion concepts are proposed which include hydrogen and electric flight.

In 2020, DLR announced in the white paper 'Zero Emission Aviation' ,together with the German Aerospace Industries Association (BDLI) [2], the strategy for a Zero Emission program. In order to prepare Europe for hydrogen and electric flight the European Commission initiated a new Alliance for Zero Emission Aviation during 2020. Current studies consider aircraft concepts using hybrid electric propulsion (HEP) whereby electric motors are applied to generate thrust and a fuel cell is installed to generate the electrical power for the motors. These have the potential to reduce the total climate impact of kerosene powered aircraft by 75-90% [3].

While the overall energy efficiency of hydrogen hybrid electric aircraft is superior to conventional aircraft, current fuel cells achieve efficiency levels of about 40-60% depending on the fuel cell type [4]. Therefore, a relevant share of the energy stored in the fuel is converted into waste heat. Under these circumstances it is necessary to install a heat exchanger integrated into a fairing cooler of an aircraft concept for heat dissipation. The assembly consisting of a heat exchanger and a fairing is referenced as the cooler in this paper.

The integration of such a cooler is an additional requirement for aircraft design and certification. DLR has identified the aerodynamic integration of the heat exchanger as a critical aspect in the clean sheet or retro-fit design of hybrid electric aircraft. In order to satisfy design heat dissipation requirements, the size of the cooler can be significant. The aerodynamical and flight mechanical requirements within an optimization process are manifold. These include, for example, the consideration of take-off and climb conditions (low velocity at high angle of attack and largest cooling condition), drag penalties due to installation effects and stability and control (S&C) requirements. Hence, it becomes relevant important to accurately assess heat exchanger designs integrated into complex aircraft geometries using numerical methods in order to reduce flight testing costs. Established CFD codes must provide physically accurate and robust methods in order to assess the

impact of the heat exchanger on the overall aircraft aerodynamics. First research flight demonstrators of novel aircraft concepts are being developed and built, for example the DLR/MTU Dornier 228 Electric Flight Demonstrator.

In order to verify the application of a numerical method for complex aircraft geometries with integrated coolers, the body-force method is applied on a generic test case. This paper analyzes a possible concept which is a pressure recovery cooler mounted below the fuselage. A visualization is shown in **Figure 1**. Similar to an engine simulation, the heat exchanger is integrated into a nacelle (cooler). The challenge with this cooler is to design the diffuser and the nozzle in a way that no flow separation occurs and the heat exchanger in a way to generate low aerodynamic drag while maintaining a high cooling efficiency. In addition, aerodynamic interactions due to the integration of this RamAir concept at the existing fuselage (in a retro-fit design) must be considered.

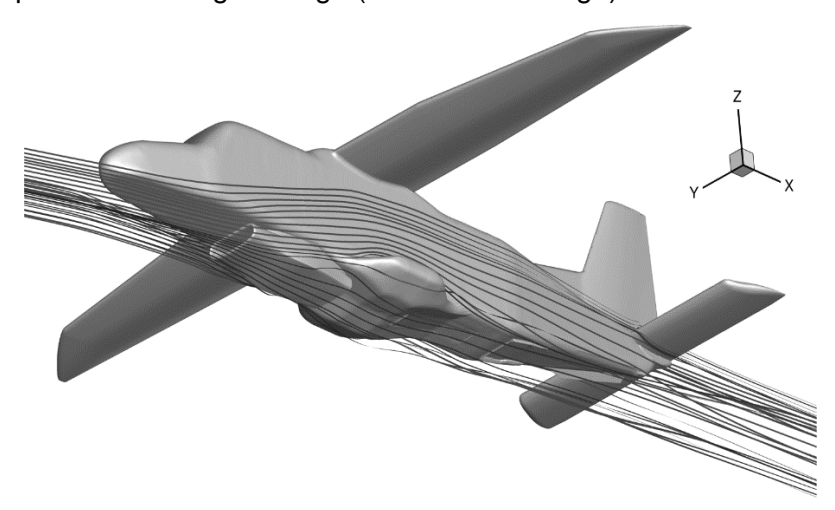


Figure 1 - Visualization of a heat exchanger concept integrated at the fuselage of the Dornier Do228.

An application of the further development of the body force method implemented in the Flowsimulator Framework of the DLR-TAU code to simulate heat exchangers will be shown in this paper. The focus is the systematic examination and continuation of previous investigations of the aerodynamic performance of an isolated nacelle, which can be used for such a fuselage-mounted heat exchanger concept. The basis for the numerical investigations is a parameterized geometry model with which the geometric changes can be made manually.

2. Numerical Methods

Previously the DLR-TAU code offered two methods capable of modeling a heat exchanger: The *Heat Exchanger* 1D boundary condition [5] and the *Actuator Disk* approach [6]. However, these methods do not fully resolve the physics of heat exchangers and were insufficiently robust for at flow conditions encountered. Therefore, an existing method for prediction of engine flows used by the DLR-TAU code [7] was modified and is applied to the simulation of heat exchangers. It is based on body force modeling using the Flowsimulator framework.

The Flowsimulator framework is coupled to the DLR-TAU code via a Python interface. The body force modeling utilizes this interface to introduce volume specific source terms into the RANS equations. In the DLR-TAU code it has been mainly applied to simulate conventional turbofan engines. Previous studies have shown that carefully defined body force source terms are able to accurately model mean aerodynamic performance in turbo-machinery flow for different flow conditions and operating points [7]. Therefore, it was assumed that the body force approach would also be suitable to simulate heat exchangers. Due to its capability to resolve three-dimensional effects, it has the potential to be superior to 1D boundary conditions or actuator disk approaches. The approach taken is conceptually similar to that adopted in other CFD codes, such as CFX, as well as OpenFOAM [8].

Experimental data for on-board cooler systems (under flight conditions) is not available and the problem at one on-flow velocity condition was also analyzed using the open-source OpenFOAM

package. This provides an additional verification case for the implementation of the body force method within the Flowsimulator package. Internal flow analysis (including heat exchanger performance estimates) are well validated in OpenFOAM in both academic and industrial applications.

The body force interface was extended according to the physics of a heat exchanger (HEX). The implementation is based on a filtering of the grid to identify the cells where HEX source terms are active. Further detailed descriptions about the source terms specified for the bode force method are summarized in [9]. The HEX is characterized by a pressure drop Δp and a heat flux \dot{q} . Three different ways to account for this pressure drop and heat flux are implemented:

1. Fixed

Constant values of the integral pressure drop Δp and the integral heat flux \dot{q} are specified by the user.

2. Lookup Table

The Flowsimulator python framework is coupled to a lookup table based on a 1D-model of the heat exchanger. The integral values of $\Delta p(p,T,U)$ and $\dot{q}(p,T,U)$ are calculated based on the average flow state one cell in front of the heat exchanger.

3. Darcy-Forchheimer approach

The pressure drop Δp and heat flux \dot{q} are calculated locally based on the Darcy-Forchheimer equation and a heat flux model.

For methods #1 and #2 a uniform distribution of the added momentum and energy within the filtered volume is assumed. Methods #2 and #3 both include an iterative approach to calculate the heat exchanger performance within the CFD simulation based on flow states through the cooler. In recent publication methods #1 and #3 in a simplified version were verified with analytical solutions as well as reference computations generated with OpenFOAM for a simple test case [10]. Earlier versions of the body force heat exchanger (BFHEX) simplified the complex flow through the heat exchanger by specifying a fixed heat flux to the volume and adding a one-dimensional source term to the momentum equation. The pressure drop Δp for a heat exchanger with the length dx was calculated from the Darcy-Forchheimer equation by specifying the permeability coefficients K and k_2 [11]:

$$-\frac{dp}{dx} = \frac{\eta}{K} u_x + \frac{\rho}{k_2} u_x^2 \tag{1}$$

where η is the dynamic viscosity, ρ is the density, and u is the velocity. This one-dimensional approach works well as long as the velocity components normal to the heat exchanger primary axis are small. However, if the normal velocity components become significant or if separations occur, this method is no longer valid. As a consequence, in this paper a three-dimensional approach is applied by extending the Darcy-Forchheimer equation to three dimensions and calculating the momentum source term \vec{f} for every cell:

$$\vec{f} = -\nabla p = [D + tr(\vec{u} \cdot I)F]\vec{u}$$
 (2)

By specifying high values for the Darcy coefficient (*D*) and Forchheimer (F) tensor coefficients in non-flow through directions, velocity components normal to the heat exchanger primary axis (flow through direction) can be removed thereby preserving flow in the heat exchanger flow through direction only. It is understood that prediction of secondary flow within a heat exchanger channel are not usually relevant within the initial system integration process. For cases where the heat exchanger flow through direction does not align with the grid coordinate system, the tensors are D and F transformed by appropriate Gallilean transformations.

The heat flux for every cell is approximated based on the local temperature T, the local velocity magnitude U, the coolant inflow temperature $T_{Coolant}$, and the reference temperature T_{∞} by the following equation:

$$f_0 = \dot{q}_{max} \cdot \frac{U}{U+b} \cdot \frac{T_{Coolant} - T}{T_{Coolant} - T_{\infty}}$$
(3)

where \dot{q}_{max} is the asymptotic value for a theoretical maximum heat flux and b defines the slope of the function for velocities in the relevant range.

The basic investigations and verifications of method #1 and #3 were summarized in [11]. This paper will be a follow-up of the investigations using the RamAir geometry and method #1 (fixed values) which were used to get a basic understanding of the impact of a heat exchanger concept on the aerodynamic performance [12] and [13]. The enhancements of the BFHEX method using the Darcy-Forchheimer equation (option #3) were presented in [14]. The focus of this paper is mainly the application and verification of method #3. In order to verify the quality of the BFHEX method.

2.1 Test Case

A generic geometry is used as test case and reference model for the cooler setup. A size for the heat exchanger (HEX) was chosen, which has a width of 1m and a height of 0.4m. **Figure 2** shows a concept of a cooler which could be integrated at the fuselage of the Dornier Do228. An isolated and symmetric cooler with a length of 4m was modelled. The HEX region (1: inlet, 2: outlet) is 0.2m long and the length of the diffuser and the nozzle is 1.9m respectively. The resulting cross-sectional area of the HEX is 0.4m² and the volume is 0.08m³. In these investigations, the cross-section area ratios of diffuser inlet to heat exchanger and nozzle outlet to heat exchanger are kept constant at 0.5.

Previous investigations have shown that the length of the diffuser is decisive to achieve good inflow conditions into the HEX without flow separations since this reduces pressure gradient across area changes between two positions in the cooler. Care must be taken to ensure that the reduction of velocity in the diffuser can take place over a sufficient length (see [12]).

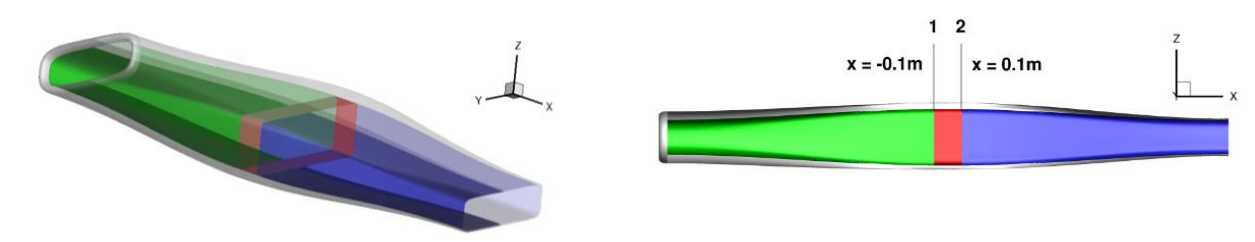


Figure 2: Generic test case geometry for the heat exchanger simulation under the fuselage

2.2 Grid Generation

The commercial grid generation software CENTAUR [15] was used to generate hybrid grids of the generic RamAir geometry. The layers normal to the surface are generated using prisms for a better resolution of boundary layers. Tetrahedra are needed to fill the computational domain to the far-field and pyramids are used for the transition between elements with quadrilateral faces and elements with triangular faces.

In order to evaluate the influence of the mesh resolution on the numerical results, a mesh refinement study is carried out. This was done prior to these investigations, with a mesh size of 8mm in the flow field [12] and [13]. The difference to the previous studies is that using the Darcy-Forchheimer method the flow state in each cell of the heat exchanger is now considered for the calculation of the source terms. Thus, it is not clear if the results obtained for the previous mesh refinement study are still valid. A new study of the mesh resolution is again necessary when applying the method #3.

Grid resolution	HEX inlet	HEX outlet	Number of grid nodes
Medium	8mm	8mm	11.93 mio.
Fine	2mm	8mm	15.13 mio.
Very fine	2mm	4mm	17.85 mio.
Ultrafine	2mm	2mm	25.24 mio.

Table 1 - Refinement settings for grid generation

For this reason, four different grids are generated in which the cell sizes from heat exchanger inlet to outlet are kept constant at 2mm and 8mm respectively and are also successively coarsened from 2mm to 8mm and from 2mm to 4mm in x-direction (see **Figure 3**). This can be realized in Centaur by a spatial source within the range of the heat exchanger (**Figure 4**), whereby the further discretization of the cooler remains the same. The number of grid nodes is summarized in **Table 1**.

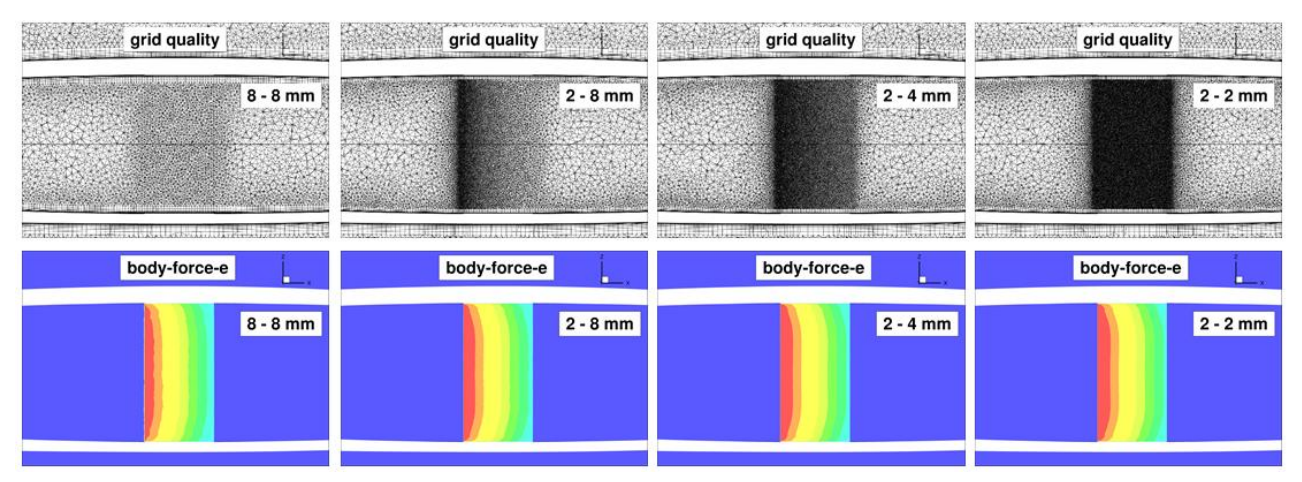


Figure 3 - Grid refinement in the region of the heat exchanger (HEX) at the top, resolution of the body force source term for the energy (heat input) at the bottom

The simulation with constant heat exchanger boundary conditions shows a different resolution of the heat flux into the flow. This is illustrated in Figure 3 by the source term for the energy (body-force-e). It also shows that less heat is emitted into the flow in the wall boundary layer area than in the middle of the flow. If the total coefficients for lift, drag and pitching moment are compared in a mesh refinement study plotted against $1/N^{2/3}$ converged solutions are obtained for all coefficients (**Figure 5**).

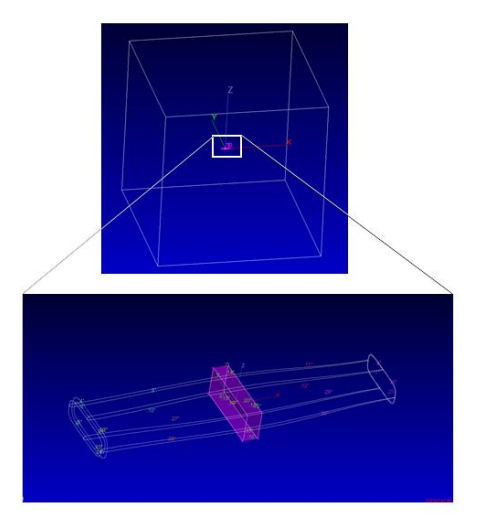


Figure 4 - Grid generation using sources for grid refinements

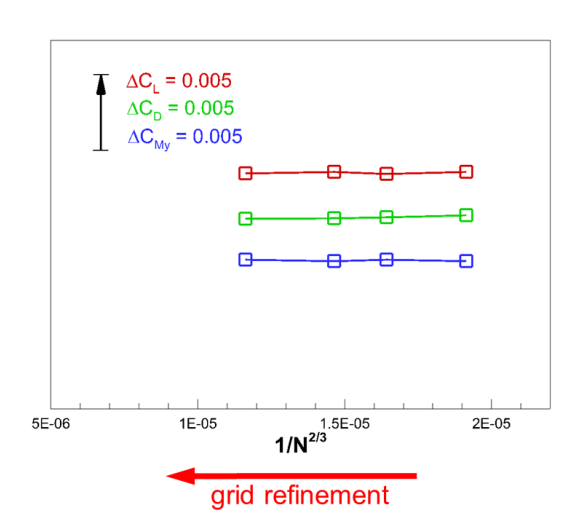


Figure 5 - Grid refinement study, U = 50m/s, $\alpha = 5^{\circ}$

This is also confirmed by the averaged flow variables through the duct center line using the four grids. The characteristic curves for static pressure, temperature, viscosity and velocity components in x-direction are almost identical except for the heat exchanger inlet (see **Figure 6**). The pressure drop is identical for all grids. However, an oscillation of the density and temperature at the beginning of the heat exchanger can be observed for the 8mm grid. This leads to a slight parallel shift in the curves of the temperature and density which also has a small upstream effect on the velocity. The difference in velocity is lower than ± 0.1 m/s. For further investigations the grid with a specified cell edge length of 8mm is used, which is sufficient for the investigations carried out here.

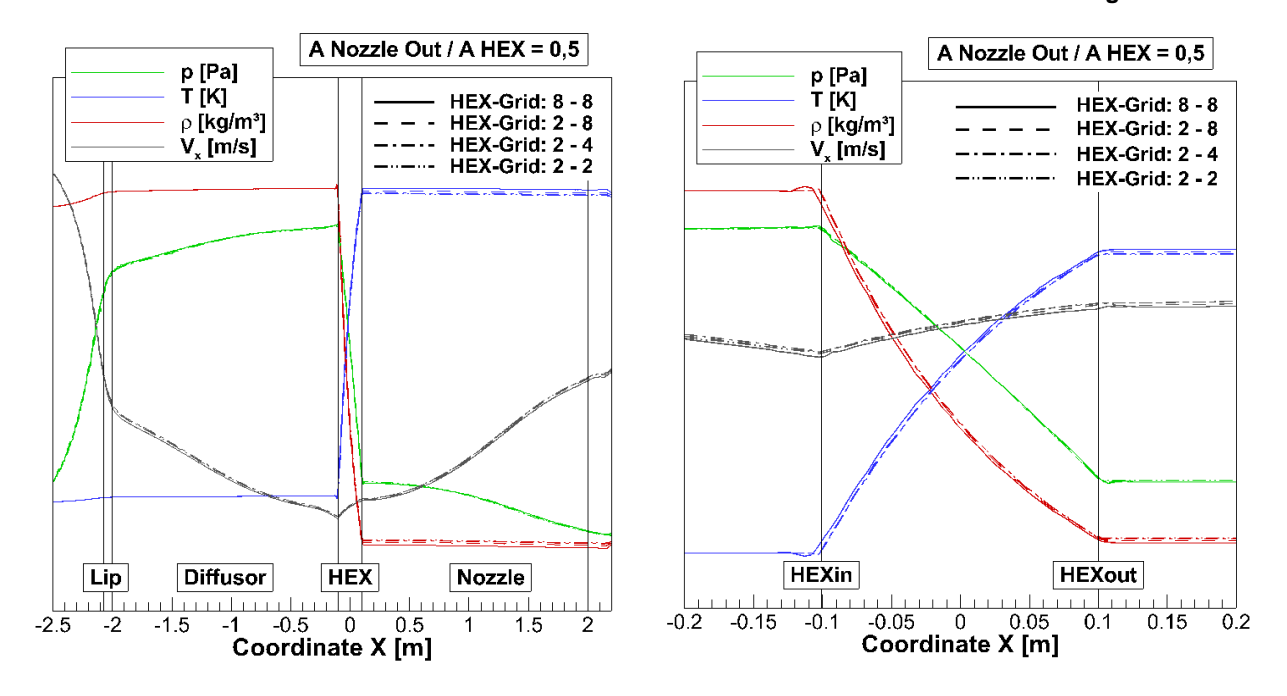


Figure 6 - Simulation with body forces approach (BFHEX) of the cooler, static pressure, temperature, viscosity and velocity in x-direction through the duct center line; entire duct (left), detailed view in the region of the heat exchanger (right); U = 50 m/s, $\alpha = 0^{\circ}$

2.3 Numerical Methods

For the numerical simulations the DLR-TAU code is applied. This method solves the compressible, time-accurate Reynolds-Averaged Navier-Stokes equations using a finite-volume formulation (see [16], [17]) and is based on an unstructured mesh data structure. As the data structure is based on the edges of the control volume, the code is independent of the type of grid cells, allowing it to handle unstructured, structured and hybrid grids composed of hexahedrons, prisms, tetrahedrons and pyramids.

The DLR-TAU code is primarily developed for external aerodynamic applications. All calculations were performed using a fully turbulent Spalart-Allmaras one-equation turbulence model [18]. A second order central differencing scheme with matrix dissipation was applied for the spatial discretization of the convective fluxes and an implicit lower upper symmetric Gauss Seidel scheme was used for time stepping.

The reference conditions used for the simulations as well as the specified HEX parameters are summarized in **Table 2**. With respect to the first investigations and verifications of the methods used ([11] and [12]) for the following simulations the values for the pressure drop and heat flux are identical.

Parameter	Value	
Flight level	0	
Reference pressure (p_{∞})	101325 Pa	
Reference temperature (T_{∞})	288.15 K	
Reference velocity (U_{∞})	50 m/s	
Heat flux (q)	100 kW	
Pressure drop (Δp)	1000 Pa	

Table 2 - Reference settings for the simulation and setup of the heat exchanger

For the application of the Darcy-Forchheimer approach (Eq. 2) and consideration of the heat flux according to Eq. 3, the necessary coefficients must therefore be determined so that the reference

values of $\Delta p = 1000$ Pa and $\dot{q} = 100$ kW are achieved. The coefficients used for configurative investigations of the cooler are shown in **Table 3**:

Coefficients	Value
D	47,1
F	3
\dot{q}_{max}	225000 W
b	15 m/s
$T_{Coolant} - T_{\infty}$	60 K

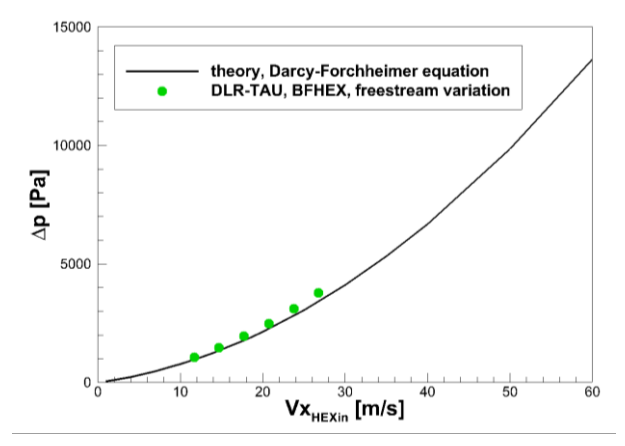
Table 3 - Reference settings for Darcy-Forchheimer and \dot{q} equation

3. Numerical Results

The focus of this paper is the application of the advanced BFHEX body force method using a 3D Darcy-Forchheimer approach [14]. This is a follow-up study, based on the investigations using the RamAir geometry, which are shown in [11] and [12]. The numerical simulations are performed at sea level and for reference conditions.

3.1 Verification of source term definition according to Darcy-Forchheimer method

The equation for the pressure drop and the heat flux depend on the velocity at the inlet of the heat exchanger. With the coefficients used in Table 3, simulations are carried out with variation of the velocity in the far-field from U = 50m/s to U = 100m/s with $\Delta U = 10$ m/s. The resulting pressure drop Δp and heat flux \dot{q} are shown in **Figure 7** as a function of the velocity in the inlet of the heat exchanger.



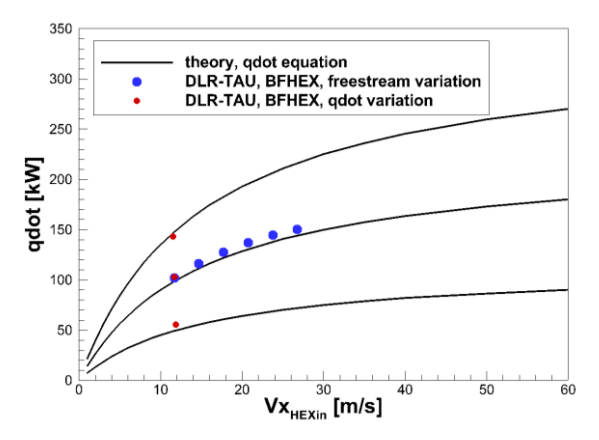


Figure 7 - Comparison of analytical specification of the pressure drop Δp (left) and heat flux \dot{q} (right) with the BFHEX simulations

The comparisons of the simulation results to the curves calculated directly from the equations show a good agreement for both, the pressure drop and the heat flux. It is recommended to fit the data within a restricted velocity range. It can be seen that the simulation with BFHEX difference against Darcy-Forchheimer increases as the velocity upper limits are approached. To verify Eq. 3, \dot{q}_{max} was also varied, which describes the asymptotic value for the theoretical maximum heat flux (red dots). This also agrees well with the analytical solution of the equation.

Figure 8 depicts the characteristic curves of static pressure, temperature, viscosity and velocity component in x-direction. The body force source term body-e, which quantifies the energy added by heat exchanger, is also included. It can be shown that relatively more heat is emitted into the flow at the beginning of the heat exchanger than at the outlet. This non-linear behavior therefore has a direct effect on all flow variables.

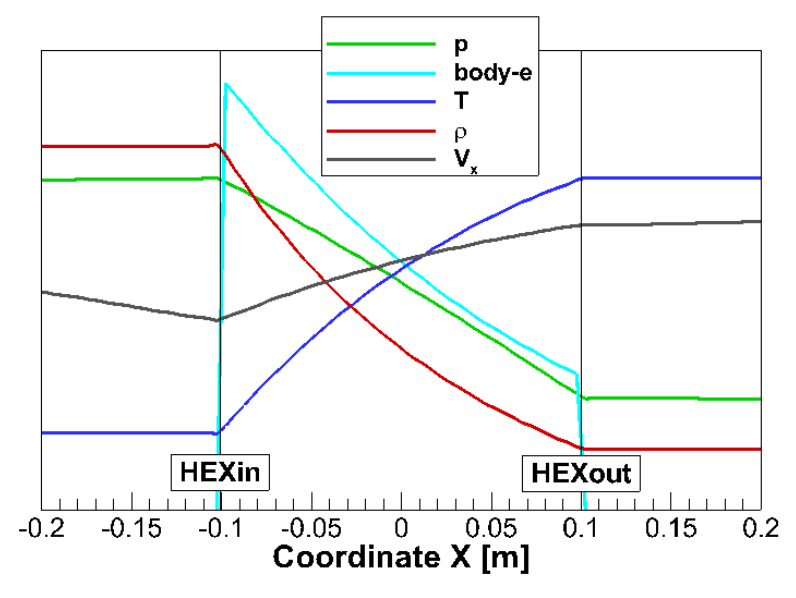


Figure 8 - General description of static pressure, body force energy source, temperature, viscosity and velocity in x-direction through the duct center line; U = 50 m/s, $\alpha = 0^{\circ}$.

3.2 Influence of source term definition for the heat flux q

As already described in Chapter 3.1, the maximum heat flux was changed by systematically varying \dot{q}_{max} (see Eq. 3). To investigate the influence on the aerodynamics of the cooler, the results are shown in **Figure 9**. Here the pressure drop Δp remains constant. As expected, the temperature difference in the heat exchanger increases as the heat flux increases. A slight decrease in the velocity at the inlet to the heat exchanger can be observed, which also means a reduction in the mass flow. This is probably caused by the higher friction loss in the flow and in the boundary layer.

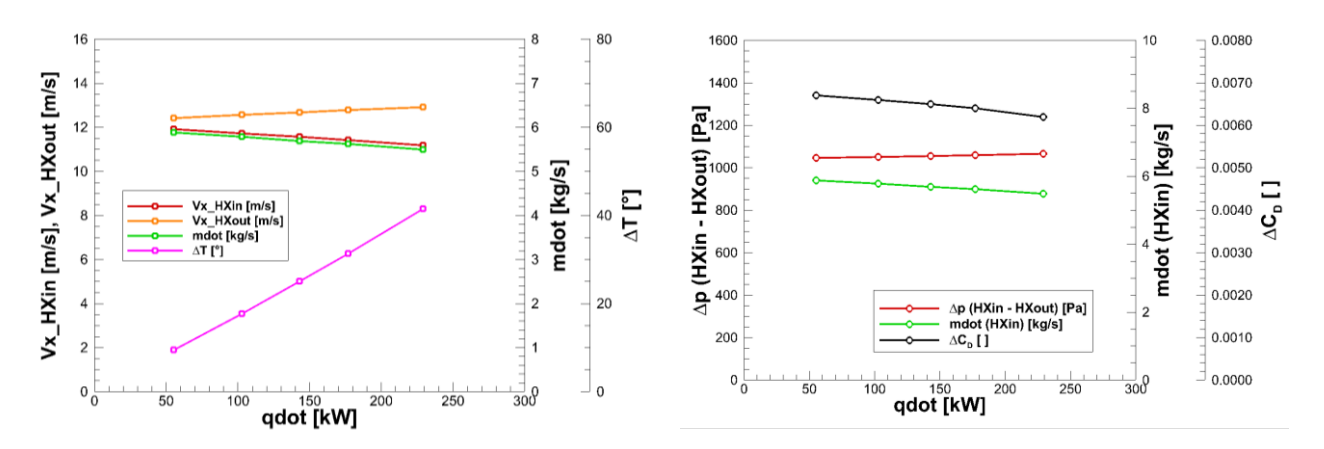


Figure 9: Influence of the heat exchanger performance on the flow conditions in the cooler for a variation of the heat flux (qdot) equation constants.

The drag ΔC_D is also shown. This is determined from the difference between the simulations with and without heat exchanger, so that only the drag component caused by the influence of the heat exchanger is shown. The simulation without heat exchanger, that means without active body force source terms, corresponds to a simulation of a flow through nacelle. It should be emphasized that increasing the heat flux by a factor of 4.1 reduces the drag component by approx. 5dcts. This is expected because energy is added to the flow and shows that it is beneficial to operate the cooler with a higher heat flux.

3.3 Comparison of different source term definitions for pressure drop Δp and heat flux ġ

In the following, the results are compared using different source term definitions for the pressure drop and the heat flux described in Chapter 2. Simulations were carried out using fixed values for Δp and \dot{q} (method #1) and also using the Darcy-Forchheimer approach and the \dot{q} equation (method #3). The flow results extracted in the center line of the duct are compared in **Figure 10**.

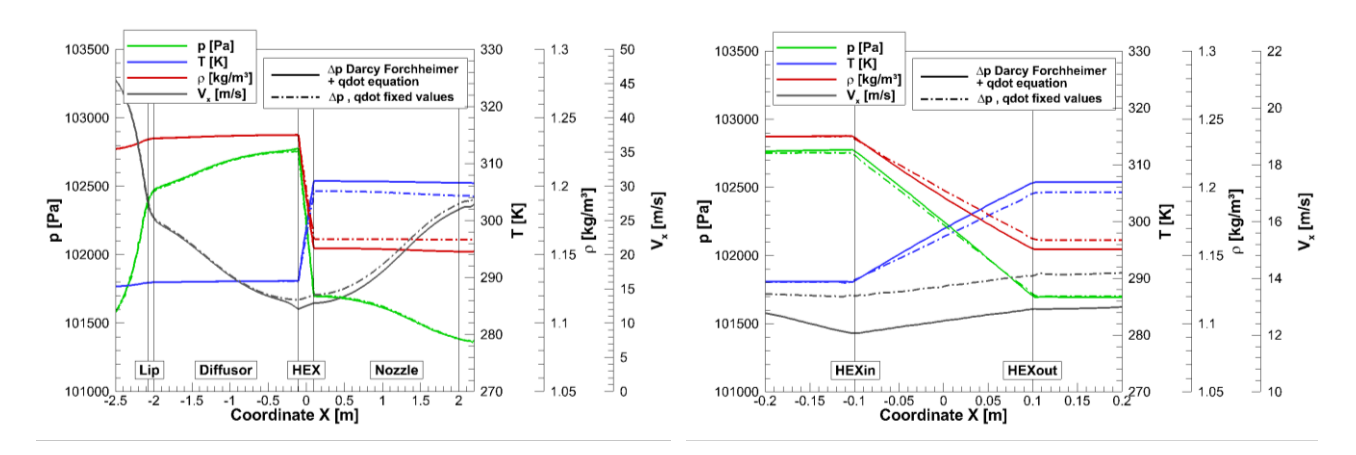


Figure 10 - Simulation with body forces approach (BFHEX) using different methods of source term specifications for pressure drop Δp and heat flux \dot{q} ; static pressure, temperature, viscosity and velocity in x-direction through the duct center line; entire duct (left), detailed view in the region of the heat exchanger (right); U = 50 m/s, $\alpha = 0^{\circ}$

It can be observed at the center line of the duct that the velocity component in x-direction in front of the HEX is lower for the Darcy-Forchheimer approach compared to method #1 with constant values. The integral values for the pressure drop are identical in both cases. However, the momentum source term is calculated for every cell with the Darcy-Forchheimer method and thus the impact of the local flow conditions are higher. As a consequence, the resulting velocity at the centerline is lower with the Darcy-Forchheimer method.

Figure 11 shows the velocity distributions for different angles of attack in x-direction in the symmetry plane (y = 0 = constant) with additional streamlines. The different methods for defining the source terms are compared. As an example, at α = 20° with both methods, the flow in the duct is aligned in x-direction and no flow separations occurs for both methods. Outside the cooler on the upper side, large detachments can already be seen. At α = 21° a large detachment area is observed in the diffuser when constant values for Δp and \dot{q} are used, while with Darcy-Forchheimer attached flow is still present. Starting with an angle of attack of α = 21.7°, a separation bubble can be detected at the inlet lip. Due to the 3D-Darcy-Forchheimer implementation and thus the alignment of the flow in x-direction through the cooler, it is therefore possible that the flow is reattached in front of the heat exchanger. This improves the inflow conditions to the heat exchanger and increases the accurate prediction of the HEX performance.

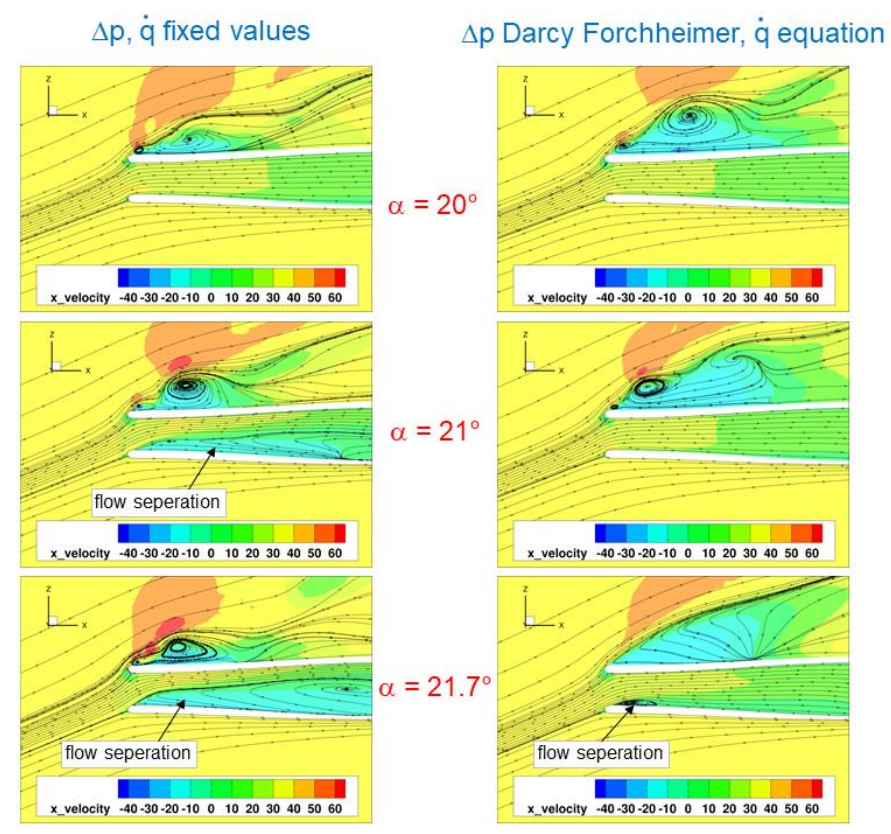


Figure 11 - Influence of different methods of the source term specifications for pressure drop Δp and heat flux \dot{q} on the flow field wrt. angle of attack of α = 20° and α = 21°; velocity distribution in x-direction in the symmetry plane with streamlines

By specifying fixed values for Δp and \dot{q} , the flow conditions also reacted sensitively to the diffuser inner contour (diffuser length and area ratio of diffuser inlet to heat exchanger size). Large cross-section expansions lead to a reduction in velocity and an increase in pressure. This allows the flow to separate more quickly and is illustrated in **Figure 12**. With the Darcy-Forchheimer method the flow remains attached and no unphysical behavior is observed even at lower velocities.

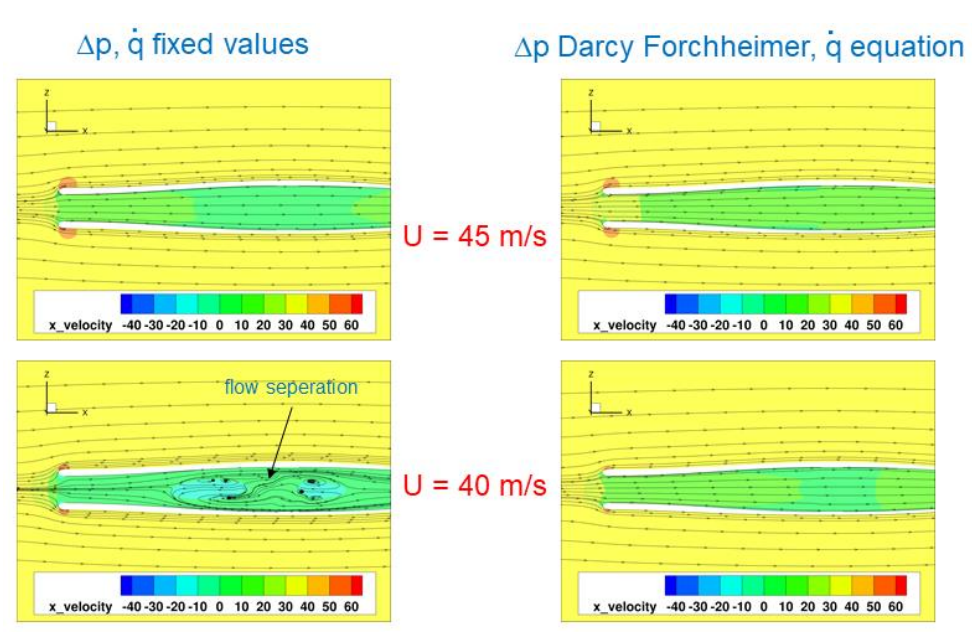


Figure 12 - Influence of different methods of the source term specifications for pressure drop Δp and heat flux \dot{q} on the flow field wrt. the freestream velocity of U = 45m/s and U = 40m/s; velocity distribution in x-direction in the symmetry plane with streamlines

3.4 Comparison of different tools for heat exchanger simulation

For a verification of the 3D Darcy-Forchheimer approach in BFHEX, the established flow solver OpenFOAM is used as a comparison. For a first analysis, the CENTAUR grid with 8mm cell size is used as a basis with the settings according to Table 2 the Darcy-Forchheimer boundary conditions for the pressure drop listed in Table 3.

It should also be noted that OpenFOAM can be considered as based on an extended Cartesian approach for which accurate computation on highly stretched boundary layer cells could be problematic. A finer mesh with a cell size of 2mm in the HEX region is available (see chapter 2.2), but is not currently used due to the high computation time. However, typical cell length scales for the volume containing the heat exchanger are typically of the finer mesh length scale (2mm) so that 8 mm is at an "upper limit".

A comparison of the averaged flow conditions through the duct center line is shown in **Figure 13**. The target values of pressure drop Δp and heat flux \dot{q} are compared with the DLR-TAU and OpenFOAM results in Table **4**.

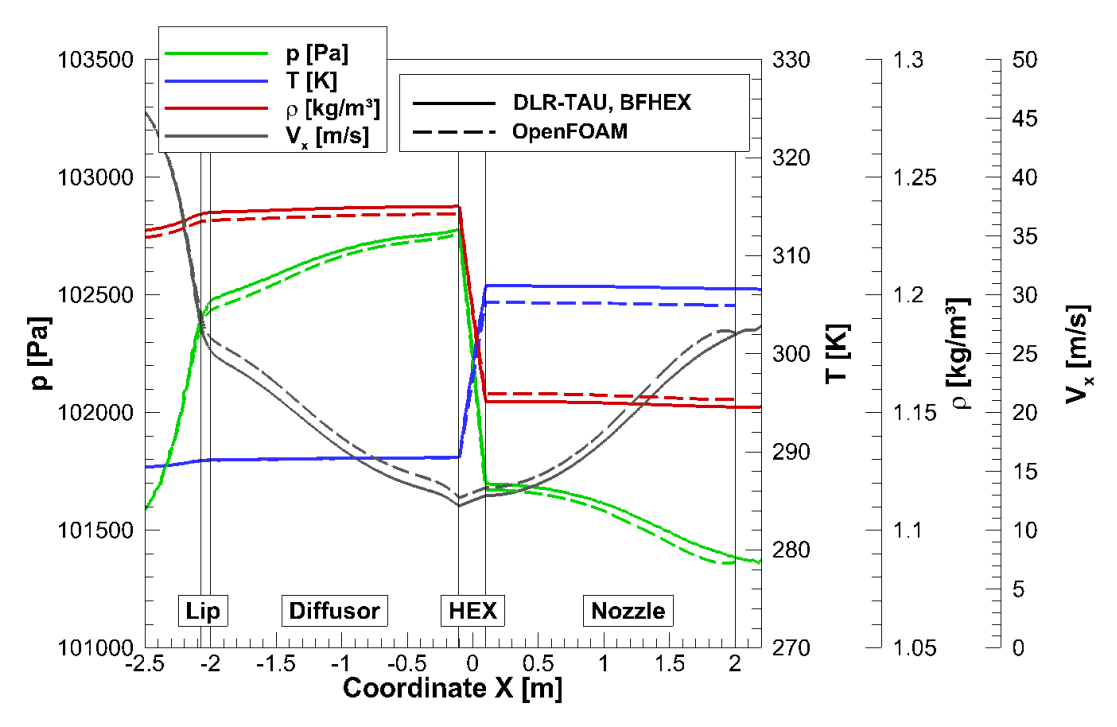


Figure 13 - Simulation of heat exchanger performance using DLR-TAU (BFHEX) and OpenFOAM Code; static pressure, temperature, viscosity and velocity in x-direction through the duct center line; entire duct; U = 50m/s, $\alpha = 0$ °

	∆p [Pa}	deviation (%)	q_dot [W]	deviation (%)
Target	-1000		100000	
DLR-TAU (BFHEX)	-1051	5,10	102908	2,91
OpenFOAM	-1065	6,50	99598	-0,40

Table 4 - Comparison of target values of pressure drop Δp and heat flux q with the DLR-TAU and OpenFOAM results

The results are qualitatively similar. The velocity curves in the area of the inlet lip show that with OpenFOAM the flow enters the diffuser at a higher velocity than with the DLR-TAU code. The calculations of the boundary layers within the tools are different. Using DLR-TAU the boundary layer flow is modeled mathematically more accurately which means that the frictional influences in the shear layers close to the wall surface are better predicted. This also has an effect on the other flow variables. Compared to the DLR-TAU results the pressure drop is approx. 1.4% higher with OpenFOAM. The velocity and therefore the mass flow are also predicted to be approx. 7% higher. In contrast, the specified heat flux of 100kW is not achieved, which is due to the reduced temperature difference and

is 3.5% lower than using BFHEX, however the OpenFOAM result is closer to the target heat rejection of 100kW.

The implementation of the Darcy-Forchheimer approach in the tools is different and therefore a deviation of approx. 6% is sufficient for these preliminary comparisons. Further investigations are still planned, in which, for example, the influences of the grid refinements and grid resolutions play a role and the definition of the heat flux must also be compared.

3.5 Influence of the nozzle length on the aerodynamic performance

To ensure good heat exchanger performance, it is important to understand the aerodynamic influences of the geometrical shape of the cooler components. For this reason, a systematic modification of the nozzle length is performed and its influence on the aerodynamics is investigated. **Figure 14** shows the systematic variation of the nozzle length in x-direction. Based on the reference size (origin \Rightarrow I = 2m (100%)) the length varied from 1.5m (75%) to 0.5m (25%).

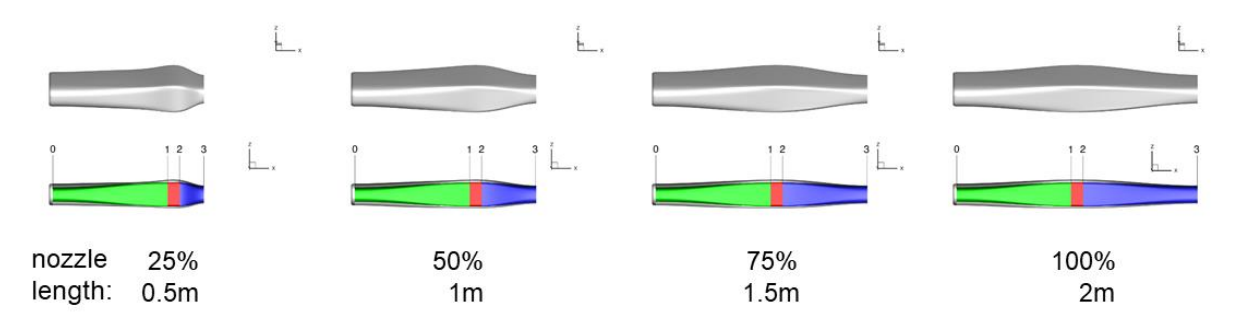


Figure 14 - Variation of the nozzle length for aerodynamic investigations

It is to be investigated how the mass flow rate and the drag change with a predefined pressure ratio and heat flux according to the different methods and settings (see Table 2 and Table 3). For this purpose, the drag of the nacelle components in the simulation without and with heat exchanger boundary condition are shown in **Figure 15**. The components include the external surfaces, the inlet lip, the diffuser, the nozzle, and the trailing edge. The sum of all components (total) is also shown. The drag due to the pressure drop (p outlet minus p inlet) at the heat exchanger is not taken into account.

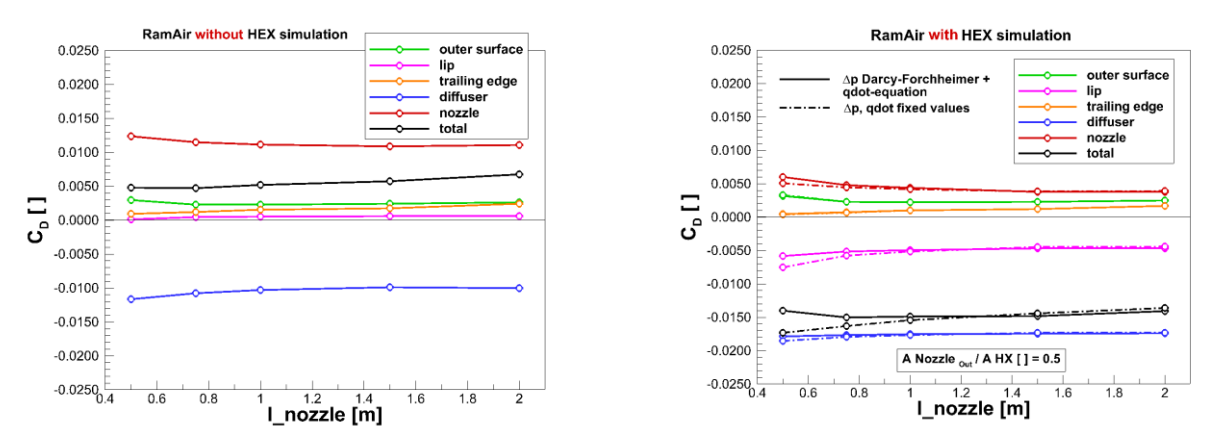
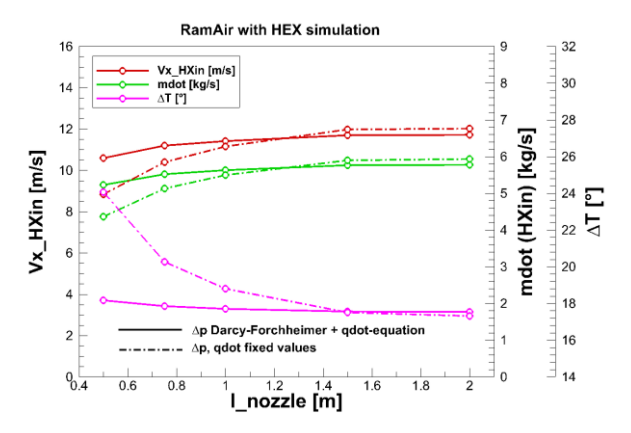


Figure 15 - Calculation without heat exchanger (left) and with heat exchanger (right), Influence of the nozzle length on the drag components of the cooler versions, U = 50 m/s, $\alpha = 0^{\circ}$.

In the case of the flow-through nacelle (left), the diffuser and the nozzle have the largest drag components and behave contrary to each other. While a positive drag is generated by the nozzle, the diffuser has a negative component. In the diffuser, the reduction of the velocity causes a force component towards the front and reduces the drag (see [12] and [13]). These effects of the diffuser and nozzle are further increased by reducing the nozzle length. The total drag decreases slightly as the nozzle is shortened due to reduced integral skin friction drag.

With the HEX boundary condition activated (see Figure 15 (right)), the drag components from the diffuser and additionally from the lip and the nozzle are reduced even further. The flow is decelerated by the pressure drop at the heat exchanger so that the upstream effect increases even more (see also [12] and [13]). In addition, the results with the different HEX modeling methods (constant values vs. Darcy-Forchheimer) for Δp and \dot{q} are shown. For short nozzles a greater reduction in drag is predicted for the lip, the diffuser and the nozzle component using constant values compared to the Darcy-Forchheimer method. This is confirmed by the total drag curves.

The differences are explained in more detail in **Figure 16**. The velocity component in x-direction in front of the HEX, the mass flow and the temperature difference between the inlet and outlet of the heat exchanger are plotted as a function of the nozzle length. While the temperature difference remains almost constant with Darcy-Forchheimer (slight increase with reduction of nozzle length), the temperature difference increases considerably with shorter nozzles using constant Δp and \dot{q} values. The inflow velocity and the mass flow behave similarly.



1100 200000 0.0080 1000 0.0070 900 800 0.0060 (HXin) [kg/s] √p (HXin - HXout) 0.0050 ₃ mdot ∆p (HXin - HXout) [Pa] 0.0030 mdot (HXin) [kg/s] 50000 0.0020 200 0.0010 ∆p, mdot fixed values 0.0000 0.6 0.8 I_nozzle [m]

Figure 16 - Simulation with heat exchanger, Influence of the nozzle length of the x-velocity and the mass flow into the inlet of the HEX, temperature difference in the HEX, U = 50m/s, $\alpha = 0^{\circ}$

Figure 17 - Simulation with heat exchanger, Influence of the nozzle length on the pressure drop, mass flow, heat flux and drag of the heat exchanger integration, U = 50m/s, $\alpha = 0^{\circ}$

Figure 17 summarizes the influence of the nozzle length on the achievable pressure drop, mass flow, heat flux and the resulting drag. As the nozzle length is reduced, the pressure difference across the heat exchanger and also the heat flux decreases slightly using Darcy-Forchheimer. As already mentioned, this is also reflected in the achievable mass flow. It should be emphasized that the total drag ΔC_D decreases significantly as the nozzle length is reduced. ΔC_D is the difference between the simulations with and without a heat exchanger. The drag due to the pressure drop (pressure at the outlet minus pressure at the inlet) of the heat exchanger is considered here.

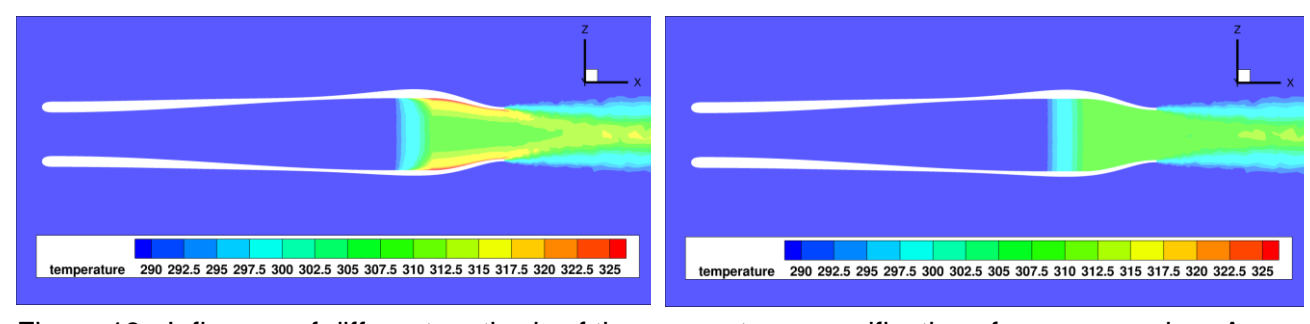


Figure 18 - Influence of different methods of the source term specifications for pressure drop Δp and heat flux \dot{q} on the temperature distribution in the symmetry plane, constant values (left), Darcy-Forchheimer and \dot{q} equation (right); nozzle length = 0.5m (25%), U = 50m/s, α = 0°

The unphysically high growth of the temperature difference when constant values are specified (see Figure 16) will be examined in **Figure 18**. The temperature distribution in the symmetry plane of the

cooler for a nozzle length of I = 0.5m is shown using the different heat exchanger modeling methods. The comparison shows that a harmonious, physical temperature distribution is obtained in the heat exchanger and in the nozzle using the 3D-Darcy-Forchheimer approach. Especially in the boundary layer, no unphysically high temperature rise can be observed, as predicted by the simpler method considering constant values.

Since the achievable heat flux and the resulting drag are different for both methods, the efficiency of the respective cooler configurations will be examined below.

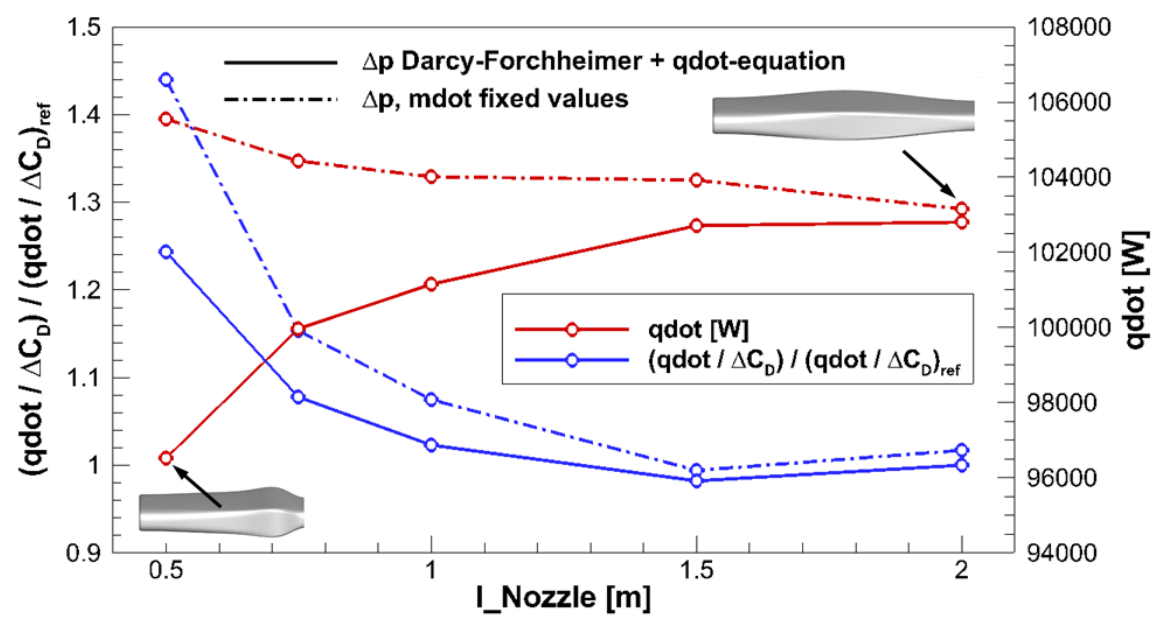


Figure 19 – Variation of the nozzle length; influence of different methods of the source term specifications for pressure drop Δp and heat flux \dot{q} ; U = 50 m/s, $\alpha = 0^{\circ}$

In **Figure 19**, the ratio of $\dot{q}/\Delta C_D$ of the respective configurations in relation to the reference geometry with a nozzle length of I=2m is plotted in addition to the achievable heat flux. Except for I=1.5m, the total heat flux decreases with the Darcy-Forchheimer as the nozzle length is reduced, but the efficiency increases up to approx. 24%. The efficiencies are even higher by using the fixed averaged values, but the results should be evaluated with caution, as the flow simulations in the nozzle predict temperatures that are unphysically high (compare Figure 18).

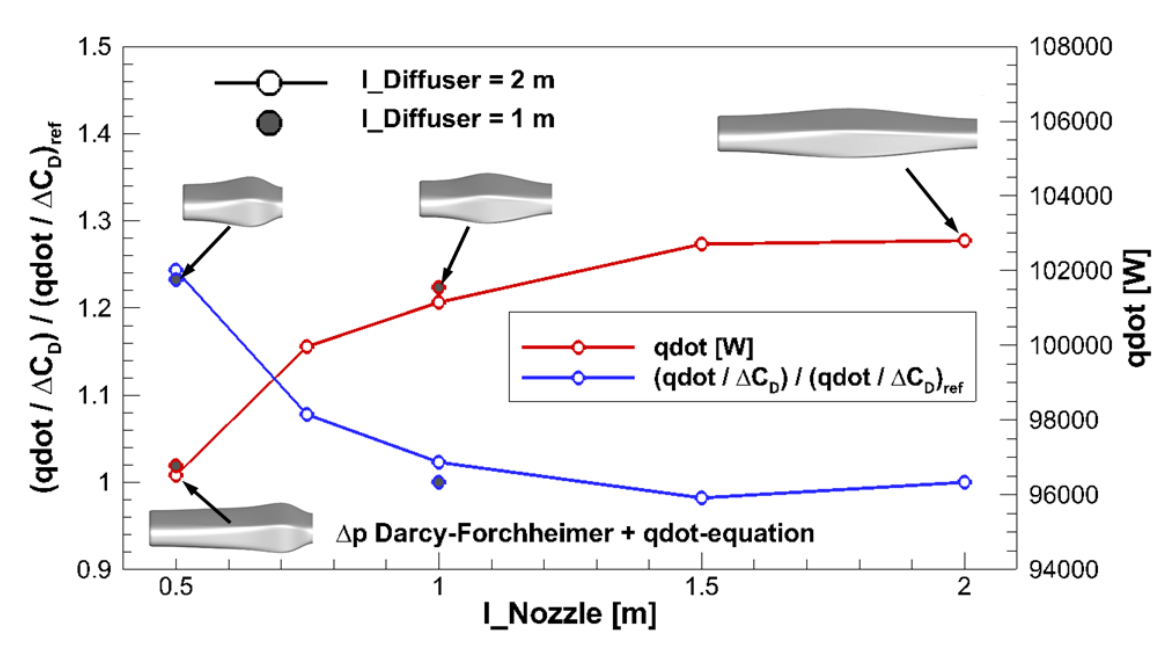


Figure 20 - Variation of the diffuser and nozzle length; Darcy-Forchheimer and \dot{q} -equation for pressure drop Δp and heat flux \dot{q} ; U = 50 m/s, $\alpha = 0^{\circ}$

Previous investigations have shown that the length of the diffuser is decisive to achieve good inflow conditions into the HEX without flow separations. Using the fixed value approach the results indicated that care must be taken to ensure that the reduction of velocity in the diffuser can take place over a sufficient length (see [12]). If the divergence angle of the diffuser and the pressure gradient due to the decrease of the velocity is high flow separations in the duct occur (compare Figure 12). For method #1 the momentum source terms do not depend on the local flow state. As a consequence, the flow is decelerated even in cells with an already small velocity magnitude, for example in the boundary layer. This leads to an overprediction of flow separations from method #1.

By using the Darcy-Forchheimer method, the flow conditions have become more physical and detachments can be avoided because no momentum is added in cells where the velocity magnitude becomes zero. Therefore, a study is to be carried out in which not only the nozzle but also the diffuser is reduced in length. **Figure 20** shows the results from simulations with heat exchangers for two variants with a diffuser length of I_Diffuser = 1m and a nozzle length of I_Nozzle = 1m and 0.5m. Compared to the configurations with long diffuser of I_Diffuser = 2m, the determined heat flux and efficiencies are slightly lower, but the variant with I_Diffuser = 1m and I_Nozzle = 0.5m also shows an increase in efficiency of up to 22%. These investigations reveal that the Darcy-Forchheimer method reproduces the physical flow conditions quite well and that new configurations can be investigated and evaluated with higher geometric variability than before.

4. Summary and Outlook

With a new tool implementation for the simulations of heat exchangers in the DLR-TAU code, a generic application case for a heat exchanger attached to the fuselage is simulated and analyzed. The main focus is the continuation of previous investigations which includes geometrical sensitivity studies of a heat exchanger - RamAir concept. The verification of the source definitions according to Darcy-Forchheimer and heat flux equation using BFHEX yields very good agreements with the theory for the velocity range examined.

Methods with different fidelity of modeling the heat exchanger were applied and compared in order to investigate the HEX performance and the aerodynamics of the cooler. It should be emphasized that increasing the heat flux by a factor of 4.1 reduces the total drag component of the cooler by approximately 5dcts. That makes it beneficial to operate heat exchangers with higher temperatures of the cooling fluid. The results shown here are geometry-dependent and may deviate depending on geometric changes.

The comparison of different methods of source term definitions for the pressure drop Δp and the heat flux \dot{q} show a better approximation of the flow physics of the heat exchanger and the cooler using the Darcy-Forchheimer approach especially for cases where separations occur in the duct of the cooler. By extending the Darcy-Forchheimer equation to three dimensions and calculating the momentum source terms for every cell the impacts of the local flow conditions can be taken into account.

The preliminary comparisons between BFHEX and OpenFOAM show qualitatively similar results. The criteria for the grid topologies used and the implementation of the Darcy-Forchheimer approach are different whereby differences in the absolute values still exist. Further investigations are necessary within the ongoing verification process.

For geometric concept studies, it is advisable to continue using the Darcy-Forchheimer approach, as the physical flow conditions are determined with greater accuracy and geometry changes can therefore be better evaluated. Using cooler concepts with shorter diffuser and nozzle lengths, it was shown that the efficiency could be increased by approx. 22% compared to the reference geometry.

For an accurate assessment of the numerical prediction method it is recommendable to perform wind tunnel tests with heat exchangers integrated into aircraft geometries in the future. With such experimental data a deeper validation of the numerical methods becomes possible.

5. Acknowledgments

This work has been funded by the German Ministry of Economic Affairs and Climate Action (BMWK) on decision of the German Parliament in the frame of the HEPS project (funding reference no. 20M1912C).

The authors would like to thank Thomas Wernsdorfer and Sebastian Spinner for the very valuable

support for the implementation and modeling of the heat exchanger. Furthermore, the authors gratefully acknowledge the valuable discussions with MTU about the numerical simulation of heat exchangers.

The authors gratefully acknowledge the scientific support and HPC resources provided by the German Aerospace Center (DLR). The HPC system CARA is partially funded by "Saxon State Ministry for Economic Affairs, Labour and Transport" and "Federal Ministry for Economic Affairs and Climate Action".

6. Contact Author Email Address

mailto: Andreas.Huebner@dlr.de

7. Copyright Statement

The authors confirm that they, and/or their company or organization, hold copyright on all of the original material included in this paper. The authors also confirm that they have obtained permission, from the copyright holder of any third party material included in this paper, to publish it as part of their paper. The authors confirm that they give permission, or have obtained permission from the copyright holder of this paper, for the publication and distribution of this paper as part of the ICAS proceedings or as individual off-prints from the proceedings.

References

- [1] Lee D S, Fahey D W, Skowron M R, Allen M R, Burkhardt U. The contribution of global aviation to anthropogenic climate forcing for 2000 to 2018. *Atmospheric Environment*, vol. 244, DOI: 10.1016 / j.atmosenv.2020.117834, 2021.
- [2] DLR, BDLI. Zero Emission Aviation German Aviation Research White Paper, 2020.
- [3] Mc Kinsey & Company, "Hydrogen-powered aviation A fact-based study of hydrogen technology,,", ISBN: 929246342X, 9789292463427, 2020.
- [4] EG&G Technical Services, Inc., "Fuel Cell Handbook," U.S. Department of Energy, 2004.
- [5] Eisfeld B, Ruetten M. A Coupled Heat Exchanger Boundary Condition for Pre-Design of Air-Intake Positions. 50th AIAA Aerospace Sciences Meeting, Nashville, TN, DOI: 10.2514/6.2012-463, 2012.
- [6] Raichle A, Melber-Wilkending S, Himisch J. A new Actuator Disk Model for the TAU Code and application to a sailplane with a folding engine. *STAB-Symposium*, DOI: 10.1007/978-3-540-74460-3_7, 2006.
- [7] Spinner S, Trost M, Schnell R. An Overview of High Fidelity CFD Engine Modeling. *AIAA SciTech*, San Diego, DOI: 10.2514/6.2022-0430, 2022.
- [8] Weller H, Tabor G, Jasak H, Fureby, Christer: A Tensorial Approach to Computational Continuum Mechanics Using Object Oriented Techniques. *Computers in Physics*, Bd. 12, pp. 620-631, DOI: 10.1063/1.168744, 1998.
- [9] Thollet W. Body Force Modeling on Fa-Airframe Interactions. PhD thesis, Institut Supérieur de l'Aéronautique et de l'Espace Toulouse, 2017.
- [10] Nield D A, Bejan A. Convection in Porous Media. Springer, ISBN: 978-1-4614-5541-7, 2013.
- [11] Kirz J, Huebner A R, Spinner S, Weinman K. Application of a body force approach for numerical heat exchanger simulations within a hybrid electric propulsion Aircraft concept. *Deutscher Luft- und Raumfahrtkongress*, DLRK2022-0202, 27.-29. September, Dresden, Germany, 2022.
- [12] Huebner A-R, Kirz J. Numerical Prediction of Heat Exchanger Performances for a Hybrid Electric Propulsion Aircraft Concept, AIAA Aviation Forum, AIAA-2023-3385, San Diego, 2023.
- [13] Huebner A-R, Kirz J. Systematic numerical investigations of a heat exchanger RAMAIR-Concept for hybrid electric propulsion Aircraft configurations. *Deutscher Luft- und Raumfahrt Kongress 2023*, 19.-21. 09. 2023, Stuttgart, Deutschland.
- [14] Kirz J, Huebner A-R. Systematic Numerical Investigations of Heat Exchangers Integrated Behind Propellers of Hybrid-Electric Propulsion Aircraft Configurations. *Deutscher Luft- und Raumfahrtkongress*, DLRK2023-610201, 19.-21.09.2023, Stuttgart, 2023.
- [15] CENTAURSOFT, http://centaursoft.com
- [16] DLR-TAU code, http://tau.dlr.de
- [17] Schwamborn D, Gerhold T, Heinrich R. The DLR-TAU Code: Recent Applications in Research and Industry. In proceedings of European Conference on Computational Fluid Dynamics, *ECCOMAS CDF* 2006, Delft, The Netherland (2006).
- [18] Spalart P R, Allmaras S R. A One-Equation Turbulence Model for Aerodynamic Flows. 30th Aerospace Sciences Meeting and Exhibit, Reno, NV, 1992.